

APPROXIMATE DYNAMIC MODEL SENSITIVITY ANALYSIS FOR LARGE, COMPLEX SPACE STRUCTURES

Timothy S. West, Senior Engineer

McDonnell Douglas Aerospace
Space Station Division, Houston, Texas

ABSTRACT

During the design of large, complex space structures, the structural analyst needs to understand the sensitivity of transient load predictions to uncertainties in critical structural vibration modes and forcing inputs. These questions arise both early in the design cycle, when models are simple and unrefined, and in the later stages of design, when models can be very complex and expensive to analyze. Therefore, the need for rapid, inexpensive assessment of these sensitivities exists at all design stages. Large, complex space structures such as International Space Station (ISS) are expensive to analyze with traditional sensitivity methods because of the tremendous number of design variables and analysis degrees of freedom. A rapid, inexpensive model sensitivity analysis method has been developed that uses modal information from a baseline model analyzed with MSC/NASTRAN Normal Modes Analysis. The method develops the system transfer function, and randomly alters the frequency and mode shape parameters of selected structural modes in the frequency domain to produce new, altered models. These new models are then used to calculate variations in transient response to known forcing inputs. The method produces approximate sensitivity information rapidly and inexpensively and can be used to assess designs at any time in the design cycle. It has been used to study ISS structural interface load sensitivities to dynamic model uncertainties. The method is presented with simple examples to illustrate its use.

INTRODUCTION

As space structures become larger and more complex, the task of creating accurate structural models becomes increasingly difficult. The International Space Station (ISS), a joint project of the United States, Russia, Japan, Canada, and the European Space Agency, is the largest and most complex space structure ever engineered. The physical structure contains many different types and shapes of interfaces and structural elements [1], and affords numerous opportunities for modelling errors and uncertainties. Variations in machining, materials, or connections, while producing small errors on smaller structures, can combine to produce significant overall errors in modelling for large structures. These errors in modelling can produce large variations in the modal properties of the models, which will produce large and possibly unacceptable variations in structural loads. Understanding the sensitivity of the predicted structural loads to both modelling uncertainties and force inputs is important to ensure proper specification of design-to loads and to develop an adequate dynamic model validation plan [2].

Typically, large, complex space structures have many degrees of freedom and contain nonlinear components. The unreduced ISS model contains nearly 2 million degrees of freedom, and also contains many nonlinear deployable structures. The large size of the problem coupled with the numerous design parameter variations that could occur create a daunting sensitivity analysis task that would be very time consuming. Further complicating sensitivity analysis, superelement and linearization techniques are often employed to reduce model complexity for modal and transient analyses [1, 3]. These reduction techniques erase the design parameters from the structural model and eliminate the possibility of using traditional sensitivity analyses which are based on varying physical properties and dimensions [4].

A model sensitivity analysis method was developed that uses modal frequencies, eigenvectors, and modal output transformation matrices (OTM) from MSC/NASTRAN (v. 68.0) Normal Models Analysis (Solution 103) [5]. The method generates a baseline modal model in the frequency domain, and alters the frequencies and mode shapes of critical structural response modes according to user defined probable variations to create new models of the structure. Assuming a well described forcing input, the method then compares the response of the new, altered models with the baseline model to determine model sensitivity. The method is simple, fast, and efficient, and effectively addresses the potential combined contributions of many design parameter variations. This method is illustrated with a concept example and an application example.

SOLUTION APPROACH

The basic goal of sensitivity analysis is to determine the effect of design parameter variations or modelling uncertainties on dynamic characteristics and structural responses [4]. Typically, design parameters are chosen and variation coefficients are computed for structural element loads or modal properties. However, when both the number of design parameters and the number of degrees of freedom are large, this process becomes very time consuming and expensive.

Another way to approach this problem is to examine the overall effect of design parameter variations. Experience in modal test/model correlation tells us two important items: 1) modal frequency uncertainties of $\pm 20\%$ are reasonable, and 2) mode amplitude uncertainties of $\pm 50\%$ are reasonable. These variations in mode frequency and amplitude represent the cumulative effect of modelling errors due to all design parameter variations. If we concentrate on varying these two modal parameters for a small number of structural modes, the problem becomes less daunting. Also, if we are dealing with large structures, we are more interested in the cumulative effect of design parameter variations and modelling assumptions than the individual effects. Therefore this approach is intuitive based on engineering judgment and experience.

The modal transfer function approach allows use of this modal parameter variation directly. We may derive the system transfer function equation by beginning with the modal equation of motion [3]. Assuming a stepped sine excitation, single input/mult output, zero initial conditions, equal damping on all modes, and mass normalized eigenvectors we have:

$$\{\ddot{\eta}\} + 2\zeta[\omega]\{\dot{\eta}\} + [\omega^2]\{\eta\} = [\phi]^T \{p\}F(t) \quad (1)$$

where:

- $\{\eta\}$ = mode displacement vector
- ζ = damping ratio
- $[\omega]$ = matrix of circular natural frequencies
- $[\phi]$ = eigenvector matrix
- $\{p\}$ = force application vector
- $F(t)$ = harmonic input disturbance

The above matrix equation describes a set of uncoupled modal equations, each of which can be considered as a single degree of freedom system:

$$\ddot{\eta}_r + 2\zeta\omega_r\dot{\eta}_r + \omega_r^2\eta_r = q_r F(t) \quad (2)$$

where:

- q_r = multiplication of the r^{th} row of $[\phi]^T$ and the force application vector $\{p\}$

The Laplace transformation of this equation yields:

$$s^2\bar{\eta}_r(s) + 2\zeta\omega_r s\bar{\eta}_r(s) + \omega_r^2\bar{\eta}_r(s) = q_r\bar{F}(s) \quad (3)$$

Rearranging:

$$\frac{\bar{\eta}_r(s)}{\bar{F}(s)} = \frac{q_r}{s^2 + 2\zeta\omega_r s + \omega_r^2} \quad (4)$$

For harmonic excitation, " $j\Omega$ " is substituted for the complex operator "s" to obtain:

$$\frac{\bar{\eta}_r(\Omega)}{\bar{F}(\Omega)} = \frac{q_r}{-\Omega^2 + j2\zeta\omega_r\Omega + \omega_r^2} = \frac{\frac{q_r}{\omega_r^2}}{1 - \left(\frac{\Omega}{\omega_r}\right)^2 + j2\zeta\frac{\Omega}{\omega_r}} \quad (5)$$

By separating q_r from the remaining terms we recognize the complex frequency response function (CFRF) [6] for a single degree of freedom system. Equation (5) then becomes:

$$\frac{\bar{\eta}_r(\Omega)}{\bar{F}(\Omega)} = H_r(\Omega, \omega_r)q_r \quad (6)$$

Equation (6) represents the generalized displacement transfer function for the r^{th} mode of the multiple degree of freedom system. To relate this generalized response to physical response we will use the mode displacement recovery method:

$$\{e(t)\} = [\text{LTM}][\phi]\{\eta(t)\} \quad (7)$$

where:

$\{e(t)\}$ = element response
 $[\text{LTM}]$ = transformation matrix from physical displacement to element load

We may multiply $[\text{LTM}]$ and $[\phi]$ and call this the output transformation matrix, $[\text{OTM}]$. If we perform the Laplace transform on (7), replace the complex operator "s" with " $j\Omega$ ", and divide through by $\bar{F}(\Omega)$, we obtain:

$$\left\{ \frac{\bar{e}(\Omega)}{\bar{F}(\Omega)} \right\} = [\text{OTM}] \left\{ \frac{\bar{\eta}(\Omega)}{\bar{F}(\Omega)} \right\} \quad (8)$$

Combining (8) with the generalized displacement transfer function for all modes of the system, and expanding to include all basic modal terms, we have:

$$\left\{ \frac{\bar{e}(\Omega)}{\bar{F}(\Omega)} \right\} = [\text{OTM}][H(\Omega, \omega_r)][\phi]^T \{p\} \quad (9)$$

Thus we may calculate the system transfer function from the modal frequencies, the mode shape vector, and the output transformation matrix of the system. All these parameters are readily available as output from a MSC/NASTRAN Normal Modes Analysis.

We may rearrange (9) to take advantage of the superposition of the individual mode CFRFs in the total system transfer function. Multiplying the CFRF matrix, the transposed eigenvector matrix, and the force application vector, we obtain:

$$[H(\Omega, \omega_r)][\phi]^T \{p\} = \begin{Bmatrix} q_1 H(\Omega, \omega_1) \\ q_2 H(\Omega, \omega_2) \\ q_3 H(\Omega, \omega_3) \\ \vdots \\ q_r H(\Omega, \omega_r) \end{Bmatrix} \quad (10)$$

We may then rewrite (9) as the product of a coefficient matrix and a column vector of the CFRFs:

$$\begin{Bmatrix} \bar{e}(\Omega) \\ \bar{F}(\Omega) \end{Bmatrix} = \underbrace{\begin{bmatrix} OTM_{11}q_1 & OTM_{12}q_2 & OTM_{13}q_3 & \dots & OTM_{1r}q_r \\ OTM_{21}q_1 & OTM_{22}q_2 & OTM_{23}q_3 & \dots & OTM_{2r}q_r \\ OTM_{31}q_1 & OTM_{32}q_2 & OTM_{33}q_3 & \dots & OTM_{3r}q_r \\ \vdots & \vdots & \vdots & \ddots & \vdots \\ OTM_{e1}q_1 & OTM_{e2}q_2 & OTM_{e3}q_3 & \dots & OTM_{er}q_r \end{bmatrix}}_{[C]} \begin{Bmatrix} H(\Omega, \omega_1) \\ H(\Omega, \omega_2) \\ H(\Omega, \omega_3) \\ \vdots \\ H(\Omega, \omega_r) \end{Bmatrix} \quad (11)$$

We can see that the system transfer function is a weighted linear combination of the CFRFs. We can therefore vary the terms in [C] and the CFRF frequencies to create new, altered models. Of course, the changes in these variables should remain within defined limits set by experience and engineering judgment. The new, altered models are intended to represent the overall effects of changes between an input forcing point and an output structural response point.

Once the altered models are created, their response to an input forcing function can be evaluated in the frequency domain. A Fast Fourier Transform (FFT) is performed on the desired transient input forcing function, and the product of the system transfer function and the forcing function is calculated to obtain the frequency domain result.

$$\bar{e}(\Omega) = G(\Omega)\bar{F}(\Omega) \quad (12)$$

An Inverse Fast Fourier Transform (IFFT) is performed on this result, and the transient domain result is compared with the transient result from the baseline model. This procedure executes very rapidly, and thousands of results can be generated within several hours on even a moderate speed computer. Once the results are generated, statistical analysis may be performed to assess the effects of model variations on element loads.

CONCEPT EXAMPLE

Consider a simple truss example to illustrate the method's ability to create new frequency domain models that accurately predict the behavior of physically altered models. In this example we will approximate a known transfer function by altering the coefficient matrix of equation (11), and will compare the response from the frequency domain approach with response from a transient analysis. Figure 1 presents a process diagram of this example, and the following paragraphs illustrate the process.

A free-free truss was created as shown in Figure 2 and called the baseline model. All members were modelled as CBAR elements [5] with initial properties shown in Table 1. A normal modes analysis was performed on the model, and the modal frequencies are shown in Table 2. The results of the normal modes analysis were used in the modal transient and transfer function analyses. In the modal transient analysis, the truss was excited at grid 1 in the Y-direction, and the Z-bending response of CBAR 504 was recovered. Figures 3 and 4 show the excitation forces applied at grid 1. The first excitation, DECSINE, was composed of two superimposed sine waves of 0.5 Hz and 1.0 Hz that exponentially decay over time. The second excitation, SQUARE, is a simple square pulse with a four second duration. The sensitivity program used the baseline normal modes analysis information to also generate a response result. Figures 5 and 6 show the bending response of CBAR 504 to both excitations, both with the modal transient solution and the transfer function based frequency domain solution. The frequency domain solution matches the modal

transient very well at initial excitation and through the peak response. Tables 3 and 4 list the top ten modal contributions for each excitation.

To generate an altered model, the radii of all CBAR elements in bay 4 of the baseline truss were arbitrarily reduced by 20%. Table 5 lists the new CBAR element properties in bay 4. A normal modes analysis was performed on this physically altered model, and the results were used to perform a transfer function analysis. Table 6 lists a comparison between the first 25 modes of the baseline model and the altered model. Mode shapes were checked to ensure a direct comparison between the modes of the two models. The changes to the baseline model produced moderate changes in the dynamic properties. Frequencies changed by a maximum of 10%, and transfer function peaks changed by 30% for more critical modes, and as much as 70% for less critical modes.

Using the same input forcing functions, the physically altered model was analyzed with the modal transient solution to calculate the true altered model response. The sensitivity program was used to generate the comparison response using the baseline modal data and the calculated mode frequency and amplitude percent differences in Table 6. The baseline transfer function was altered by changing the coefficient matrix and frequencies of the CFRFs for the top ten modes listed in Tables 3 and 4 for the respective input forcing functions. A comparison of the results of both solutions for both inputs is shown in Figures 7 and 8. Again, the two solution methods match very well at initial excitation and through the peak response. Table 7 shows that the percent difference between the frequency domain solution and modal transient solution maximum and minimum response peaks is less than 10%. Therefore, this method can be used to form altered models that accurately predict transient load variations.

APPLICATION EXAMPLE

In sensitivity analysis of large, complex space structures, we are interested in the effects of many modelling uncertainties throughout the structure. These modelling uncertainties are assumed to be random in nature and may combine to significantly change the modal properties of the structure, which may in turn significantly change structural loads predictions. The above concept may be employed to produce loads results for altered models, and these results may be statistically analyzed to determine load sensitivity to model uncertainties prior to test/model correlation. Figure 9 illustrates the procedure used in practical application of this concept. To demonstrate the accuracy and speed of this procedure, the simple truss in Figure 2 was analyzed both in a brute force analysis (modal and transient analysis of each model variation) and with the sensitivity analysis procedure, and results from the two analyses were compared.

Brute Force Analysis

Fifty physically altered models of the simple truss were created by independently, randomly varying the radii of all the CBAR elements. These radii were randomly varied according to a normal distribution with zero mean (μ) and 10% standard deviation (σ). The modal properties of the physically altered models were calculated in a normal modes analysis. The input forcing function DECSINE was applied to the physically altered models as in the concept example, and transient loads were calculated for CBAR 504. Histograms of these results are presented in Figures 10-12 in comparison with the sensitivity analysis results. The analysis was computationally intensive because a new eigensolution and transient response solution was calculated for each new model.

Sensitivity Analysis

As shown in Figure 9, the inputs to the sensitivity program are the baseline modal properties, the baseline transient results and important response modes, the frequency domain transformed forcing function, and the mode frequency and amplitude variation parameters. The baseline modal

properties were calculated for the baseline model in a normal modes analysis. The input forcing function DECSINE was applied to the baseline model as in the concept example, and the transient results of CBAR 504 were recovered. The important response modes were calculated in a modal contribution analysis of these transient results. The frequency domain transformed forcing function was calculated by applying an FFT to the input forcing function DECSINE. To develop the modal frequency and amplitude variations for this example, the altered eigenvectors from the brute force analysis were compared with the baseline model to ensure a direct comparison of transfer functions. Transfer functions were then generated for each model and were compared with the baseline model transfer function to determine mode frequency and magnitude variation. The sample statistical frequency and magnitude variations of the important response modes were calculated as $\mu=0$ and $\sigma=3$ Hz, and $\mu=0$ and $\sigma=31$, respectively, and these parameter variations were used in the sensitivity analysis. The parameter variations were approximately normally distributed.

In the sensitivity analysis, 1000 samples of loads were calculated for the bending, shear, and torsion of CBAR 504 by randomly varying the mode frequency and amplitude on the critical modes listed in Table 3 according to a normal distribution with μ and σ as listed above. Histograms of the results of this sensitivity analysis are shown in Figures 10-12 in comparison with the brute force analysis results. We can see that for all three responses, the distribution of loads is very similar. The sensitivity analysis was conducted in approximately 3% of the time needed for the brute force analysis, and produced 950 more results cases than the brute force analysis.

The main question the user faces in the above procedure is how to define and use the mode frequency and amplitude variation parameters in the sensitivity program. In this example, the variation limits were determined statistically from the brute force example to achieve a good results comparison. However, in most cases engineering judgment must be used to determine a reasonable range of variation. As stated earlier, test/model correlation experience tells us that modal frequency variations of $\pm 20\%$ are reasonable, and mode amplitude variations of $\pm 50\%$ are reasonable. These can provide adequate boundaries in most analyses to investigate dynamic load sensitivities to model uncertainties prior to test/model correlation.

CONCLUSIONS

An accurate and computationally efficient procedure for approximate dynamic model sensitivity analysis of large, complex space structures has been presented. The procedure utilizes modal data from a MSC/NASTRAN Normal Modes Analysis and generates altered system transfer functions for use in predicting structural loads sensitivity to model changes and modelling uncertainties. A concept example and an application example were presented to demonstrate the accuracy and feasibility of the method.

By varying the modal frequency and amplitude of a baseline transfer function to approximate a known, altered transfer function, accurate transient results were produced for two different types of force input using this frequency domain approach. A comparison of the peak results from the transient and frequency domain analyses yielded a difference of less than 10%.

Random variation of modal frequency and amplitude of baseline transfer functions allowed rapid generation of altered models and rapid analysis of structural loads sensitivity. This data may be produced at any point in the design cycle, and is useful in both design evaluation and structural model validation planning. Cost of generating this data is low even for large models possessing millions of degrees of freedom.

ACKNOWLEDGMENTS

The development of the procedure described herein was conducted under Contract HX 3222 for Boeing Defense & Space Group. The author wishes to thank H. H. Doiron, H. M. Kim, and S. L. Shein of McDonnell Douglas Aerospace - Space Station Division for suggestions and support.

REFERENCES

- [1] *International Space Station Alpha March 1995 Incremental Design Review On-Orbit Transient Loads Integrated Finite Element Model Generation Report*. MDA Document Number A96-J112-STN-M-BNM-9400074. November 15, 1994
- [2] *Structural Design and Verification Requirements, Rev. B*. NASA Document Number SSP30559. June, 1994.
- [3] Craig, Roy R., Jr., *Structural Dynamics, An Introduction to Computer Methods*, John Wiley & Sons, Inc., 1981.
- [4] *MSC/NASTRAN Design Sensitivity and Optimization User's Guide, Version 68*, The MacNeal-Schwendler Corporation, Los Angeles, CA, May 1994.
- [5] *MSC/NASTRAN Reference Manual, Version 68*, The MacNeal-Schwendler Corporation, Los Angeles, CA, April 1994.
- [6] Meirovitch, Leonard, *Analytical Methods in Vibrations*, Macmillan Publishing Company, Inc., 1967.

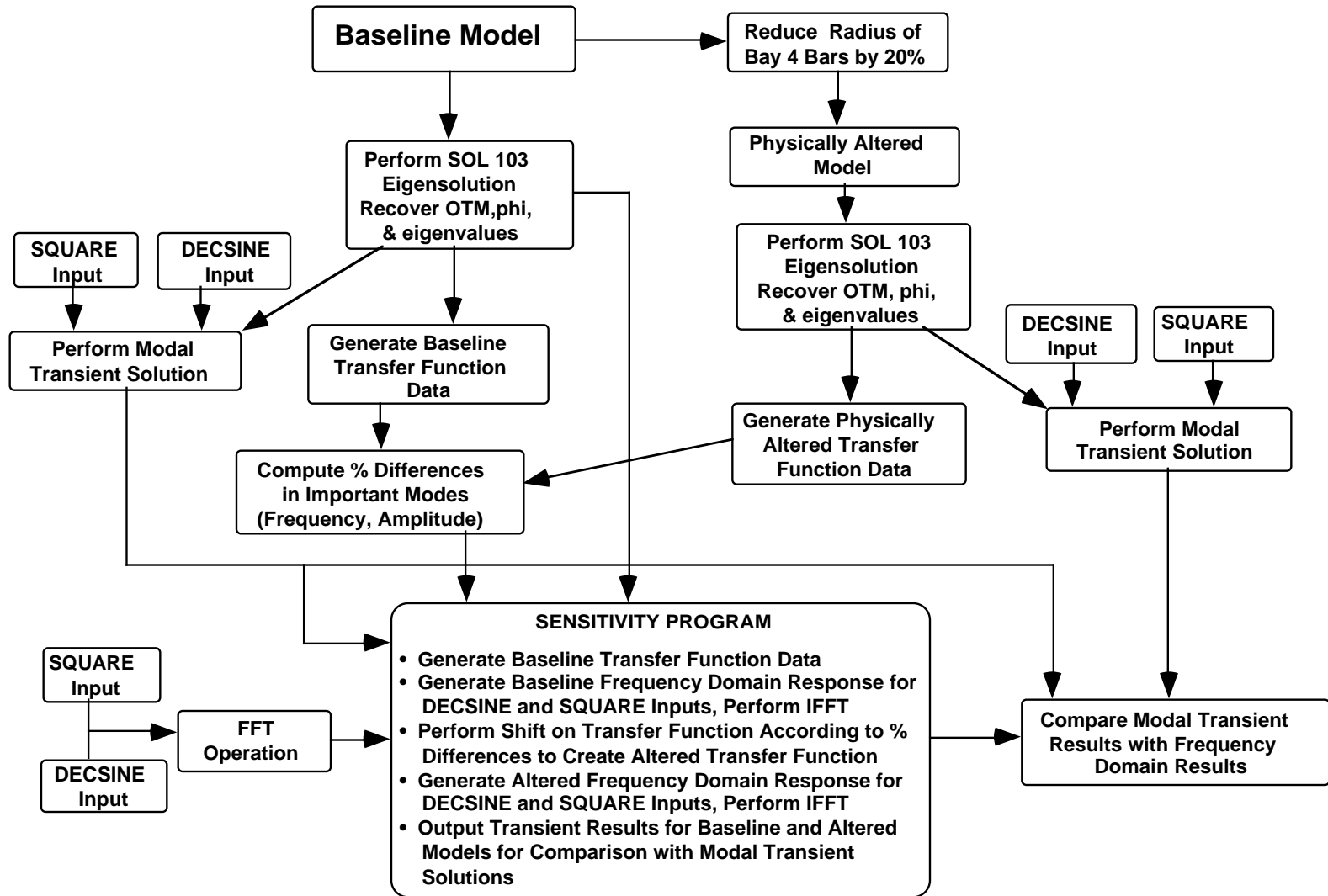


Figure 1: Flow Diagram for Concept Example

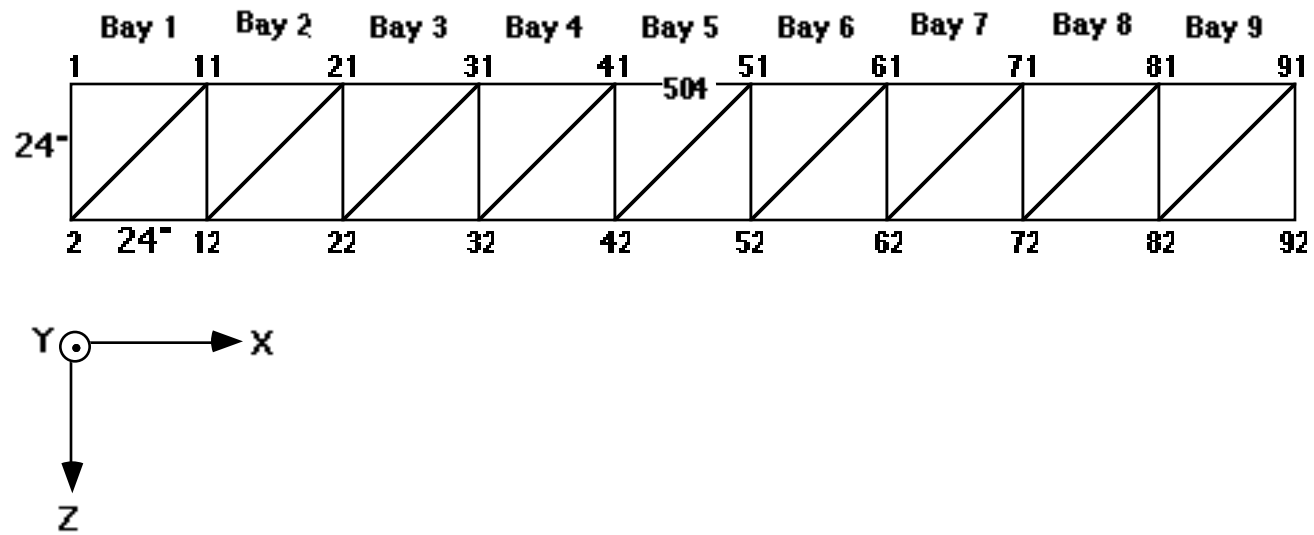


Figure 2: Simple 9-Bay Truss

Table 1: CBAR and Material Properties for Baseline Truss

Parameter	Value
Area, in ²	0.00785
I ₁ , in ⁴	4.91E-06
I ₂ , in ⁴	4.91E-06
J, in ⁴	9.82E-06
Young's Modulus, lb/in ²	29.5E+06
Shear Modulus, lb/in ²	11.5E+06
Poisson's ratio	0.287
Density, lb/in ³	0.283

Table 2: First 25 Free-Free Modal Frequencies for Baseline Truss

Mode Number	Frequency (Hz)	Description
1	3.14E-07	Rigid Body Mode
2	4.33E-07	Rigid Body Mode
3	5.12E-07	Rigid Body Mode
4	4.51E-05	Rigid Body Mode
5	5.31E-05	Rigid Body Mode
6	9.07E-05	Rigid Body Mode
7	2.65E-01	1 st Bending (Z)
8	7.18E-01	2 nd Bending (Z)
9	8.01E-01	1 st Torsion (X)
10	1.38E+00	3 rd Bending (Z)
11	1.61E+00	2 nd Torsion (X)
12	2.24E+00	4 th Bending (Z)
13	2.42E+00	3 rd Torsion (X)
14	3.25E+00	4 th Torsion (X)
15	3.26E+00	5 th Bending (Z)
16	4.07E+00	5 th Torsion (X)
17	4.38E+00	6 th Bending (Z)
18	4.92E+00	6 th Torsion (X)
19	5.45E+00	High Order Bending (Z)/Torsion (X)
20	5.78E+00	High Order Bending (Z)/Torsion (X)
21	6.31E+00	High Order Bending (Z)/Torsion (X)
22	6.52E+00	High Order Bending (Z)/Torsion (X)
23	6.92E+00	High Order Bending (Z)/Torsion (X)
24	9.65E+01	1 st Bending (Y)
25	2.03E+02	2 nd Bending (Y)

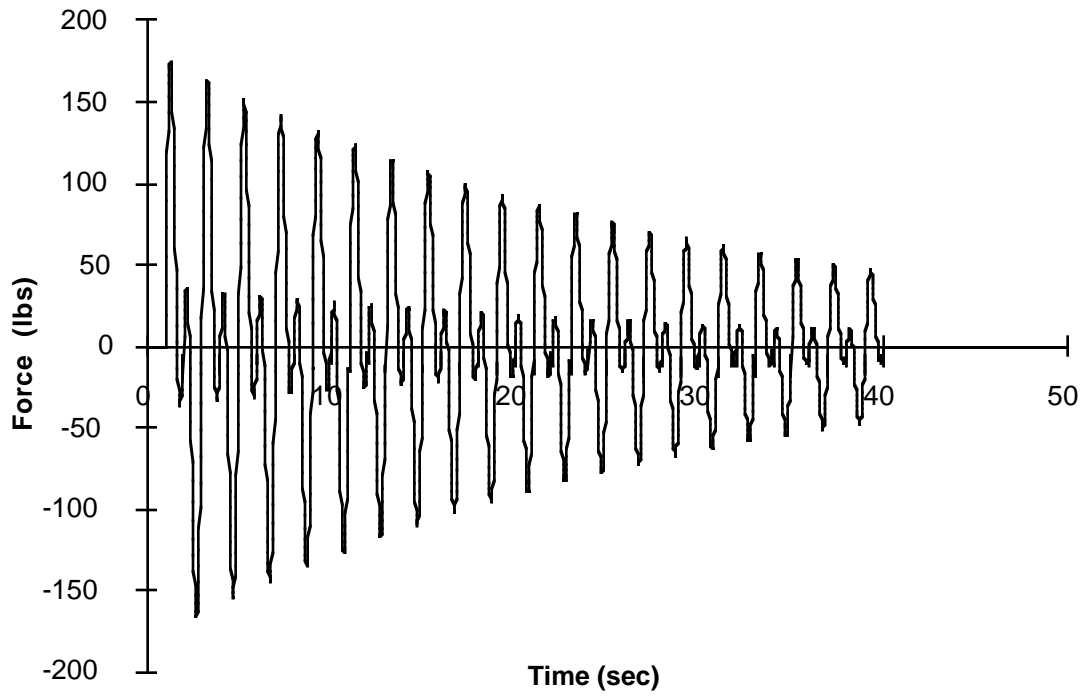


Figure 3: Exponentially decaying 0.5 Hz and 1.0 Hz sine wave input - DECSINE

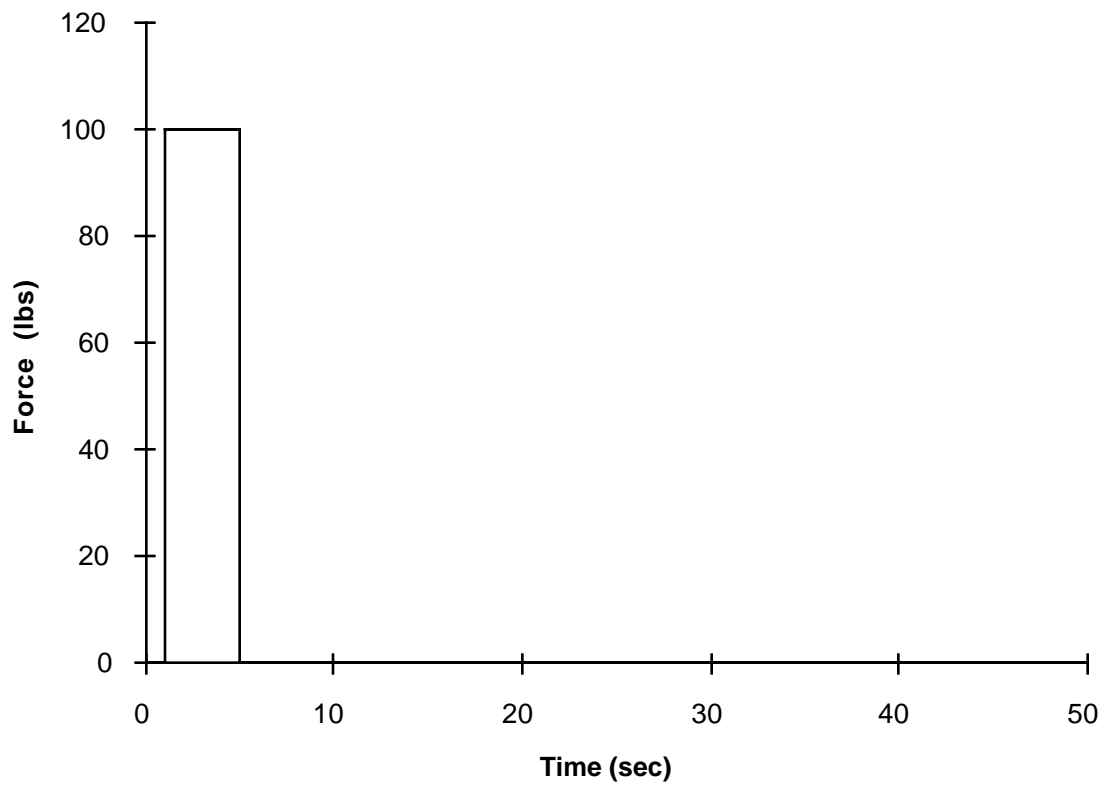


Figure 4: Square wave input - SQUARE

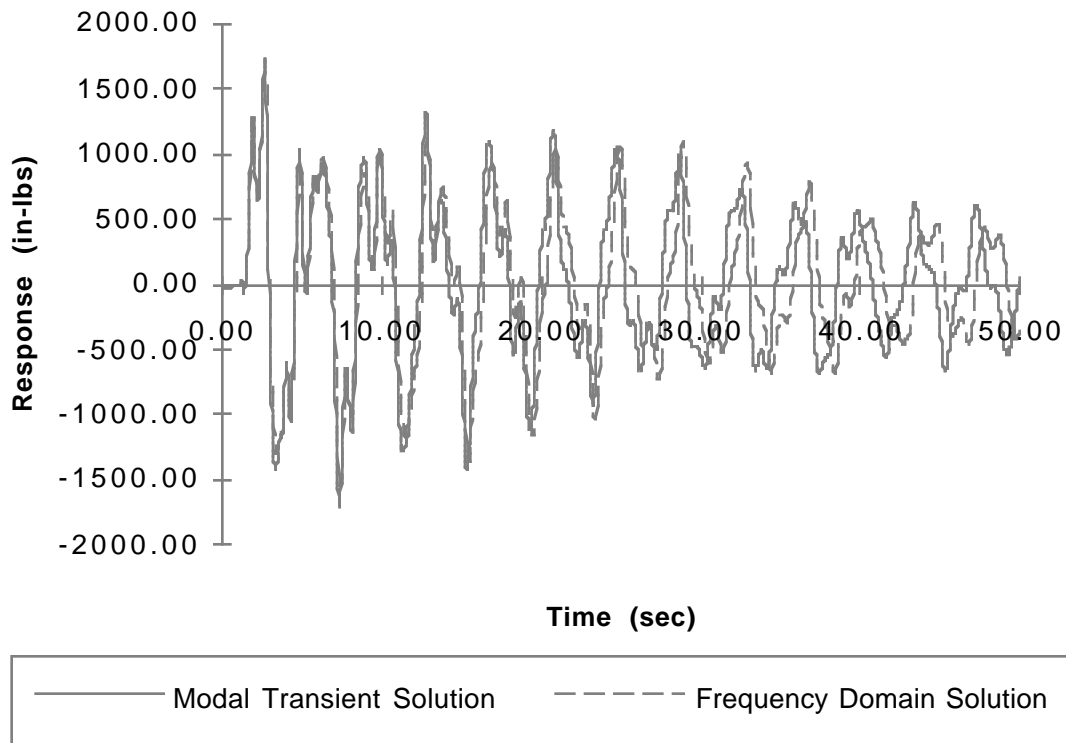


Figure 5: Baseline Truss CBAR 504 Response to DECSINE Input
(Modal Transient and Frequency Domain Solutions)

Table 3: Top Ten Modal Contributions for DECSINE Input

Mode Number	Frequency (Hz)	Contribution	Percent
7	0.26535	809.37	47.01
10	1.38155	670.85	38.97
9	0.80066	163.86	9.52
13	2.42261	137.17	7.97
15	3.25903	-118.70	-6.89
8	0.71782	117.02	6.80
12	2.23817	-105.42	-6.12
17	4.37801	93.61	5.44
16	4.07432	-76.61	-4.45
19	5.45210	68.29	3.97
TOTAL		1759.43	102.20

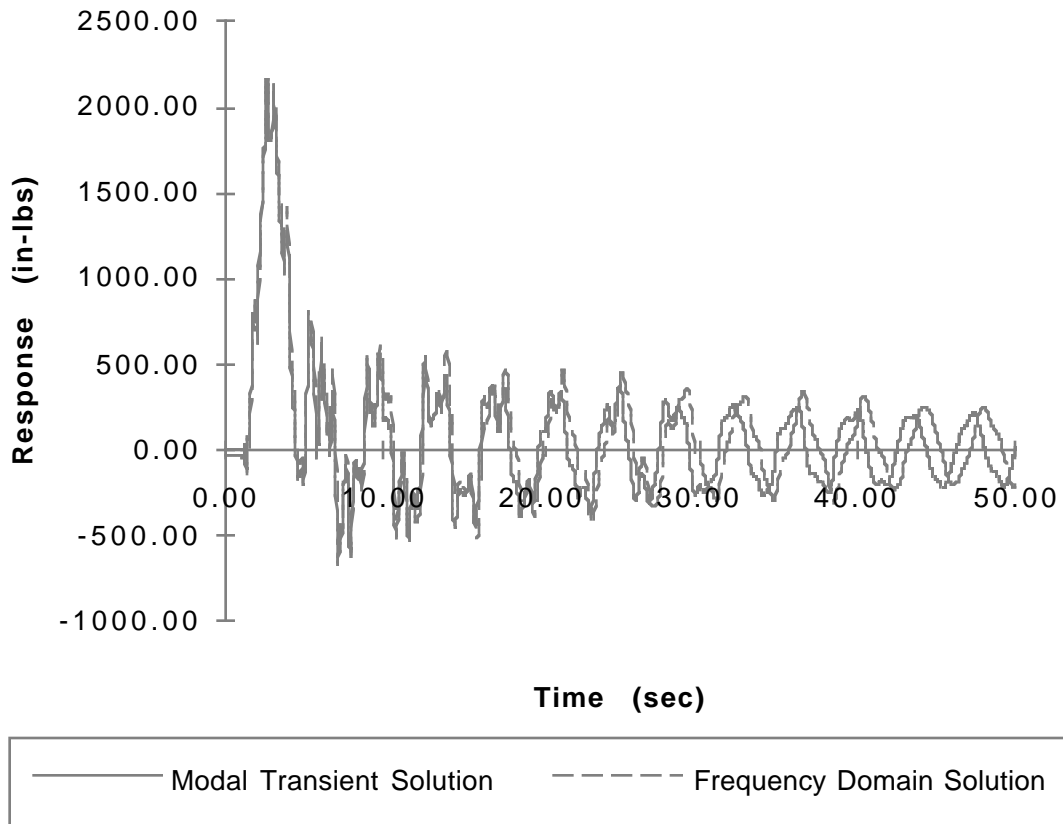


Figure 6: Baseline Truss CBAR 504 Response to SQUARE Input
(Modal Transient and Frequency Domain Solutions)

Table 4: Top Ten Modal Contributions for SQUARE Input

Mode Number	Frequency (Hz)	Contribution	Percent
7	0.26535	1954.29	90.47
9	0.80066	206.81	9.57
10	1.38155	-141.59	-6.55
12	2.23817	135.20	6.26
16	4.07432	85.52	3.96
8	0.71782	-80.95	-3.75
15	3.25903	63.89	2.96
11	1.60725	46.99	2.18
19	5.45210	-34.04	-1.58
14	3.24500	-31.17	-1.44
TOTAL		2204.95	102.07

Table 5: Altered CBAR and Material Properties for Bay 4 of Truss

Parameter	Value
Area, in ²	0.00503
I ₁ , in ⁴	2.01E-06
I ₂ , in ⁴	2.01E-06
J, in ⁴	4.02E-06
Young's Modulus, lb/in ²	29.5E+06
Shear Modulus, lb/in ²	11.5E+06
Poisson's ratio	0.287
Density, lb/in ³	0.283

Table 6: Comparison of First 25 Free-Free Modal Frequencies

Mode Number	Baseline Frequency (Hz)	Altered Frequency (Hz)	% Difference	Baseline System TF Peak	Altered System TF Peak	% Difference
1	3.14E-07	4.44E-07	n/a	n/a	n/a	n/a
2	4.33E-07	4.45E-07	n/a	n/a	n/a	n/a
3	5.12E-07	4.95E-07	n/a	n/a	n/a	n/a
4	4.51E-05	5.74E-05	n/a	n/a	n/a	n/a
5	5.31E-05	6.20E-05	n/a	n/a	n/a	n/a
6	9.07E-05	8.30E-05	n/a	n/a	n/a	n/a
7	2.65E-01	2.37E-01	-10.41	-521.78	-542.46	3.96
8	7.18E-01	6.85E-01	-4.60	81.80	99.63	21.80
9	8.01E-01	7.26E-01	-9.40	-82.95	-111.62	34.56
10	1.38E+00	1.36E+00	-1.21	79.60	82.91	4.16
11	1.61E+00	1.60E+00	-0.86	-13.51	-14.16	4.81
12	2.24E+00	2.14E+00	-4.39	-41.49	-46.73	12.63
13	2.42E+00	2.37E+00	-1.88	37.99	43.59	14.74
14	3.25E+00	3.12E+00	-4.10	-9.32	-2.79	-70.06
15	3.26E+00	3.16E+00	-3.02	-16.61	-26.76	61.11
16	4.07E+00	4.06E+00	-0.23	-26.56	-24.46	-7.91
17	4.38E+00	4.28E+00	-2.35	24.35	24.72	1.52
18	4.92E+00	4.72E+00	-4.04	-15.50	-7.40	-52.26
19	5.45E+00	5.27E+00	-3.35	21.03	14.87	-29.29
20	5.78E+00	5.64E+00	-2.50	-	-	-
21	6.31E+00	6.10E+00	-3.40	-	-	-
22	6.52E+00	6.29E+00	-3.47	-	-	-
23	6.92E+00	6.69E+00	-3.37	-	-	-
24	9.65E+01	9.38E+01	-2.75	-	-	-
25	2.03E+02	1.98E+02	-2.47	-	-	-

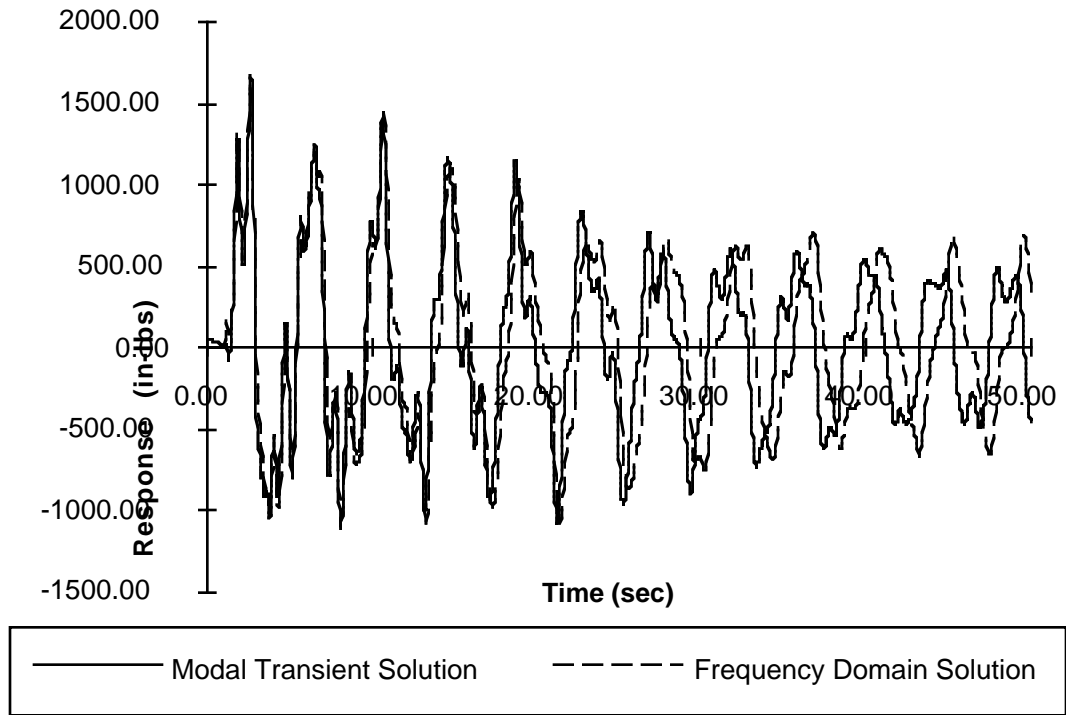


Figure 7: Altered Truss CBAR 504 Response to DECSINE Input (Modal Transient and Frequency Domain Solutions)

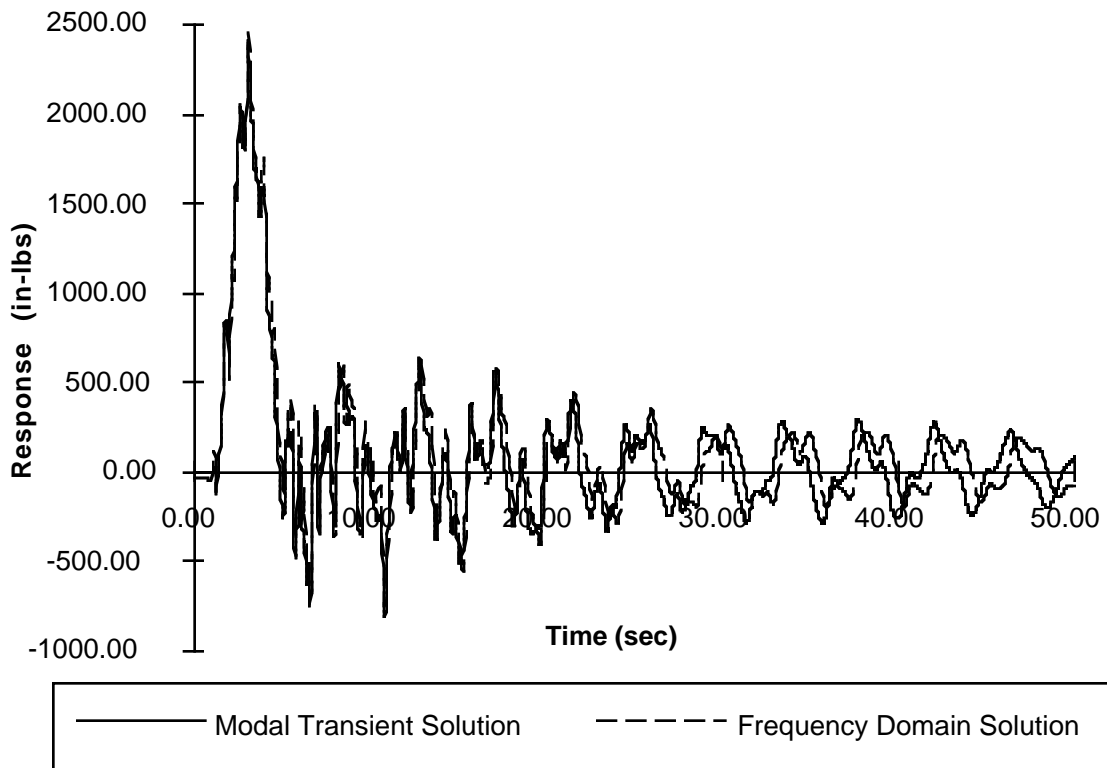


Figure 8: Altered Truss CBAR 504 Response to SQUARE Input (Modal Transient and Frequency Domain Solutions)

Table 7: Comparison of Peak Results for Solution Methods on Altered Model

	Maximum Response % Difference	Minimum Response % Difference
DECSINE Input	-4.50	-2.33
SQUARE Input	1.73	-7.48

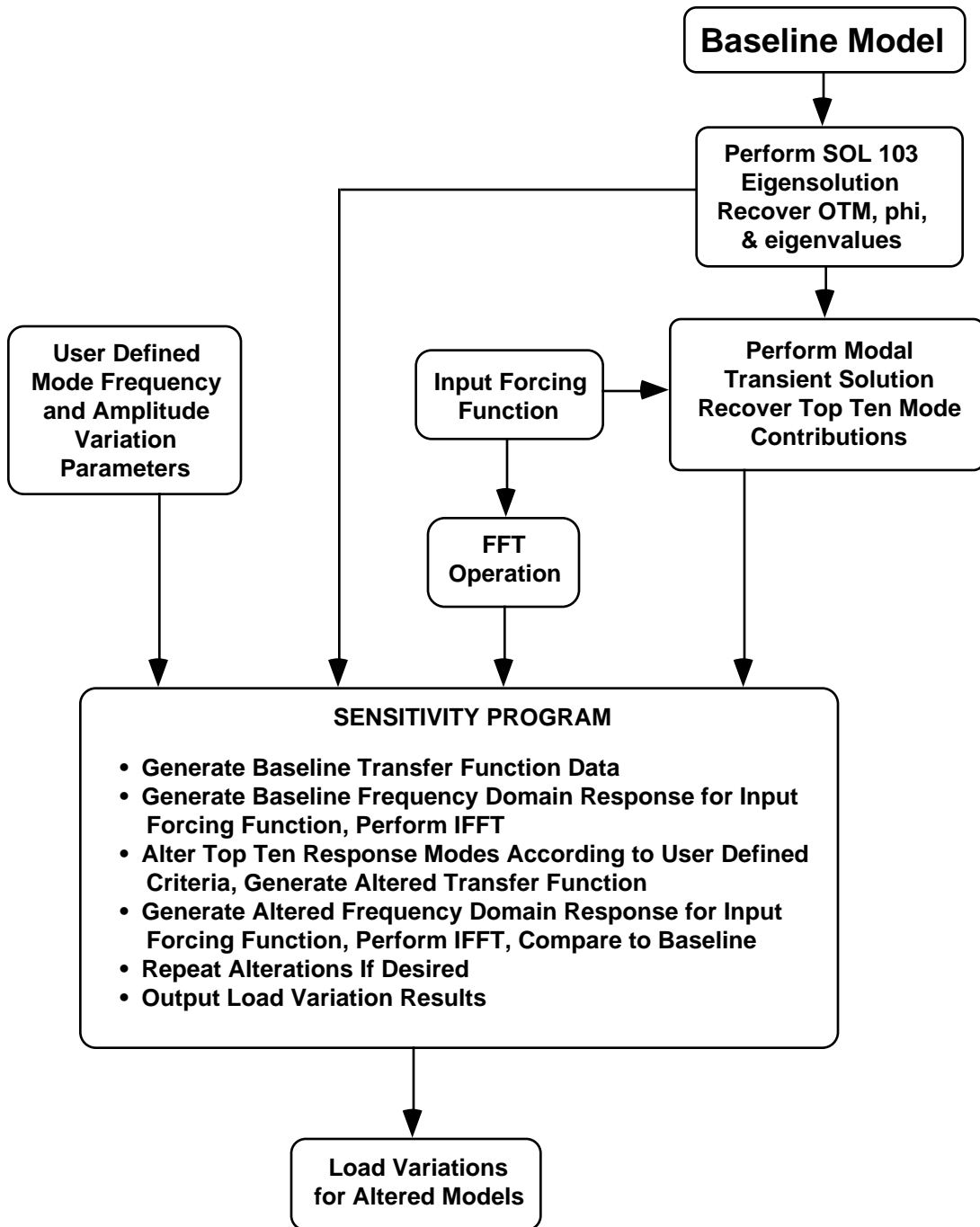


Figure 9: Flow Diagram for Application Example

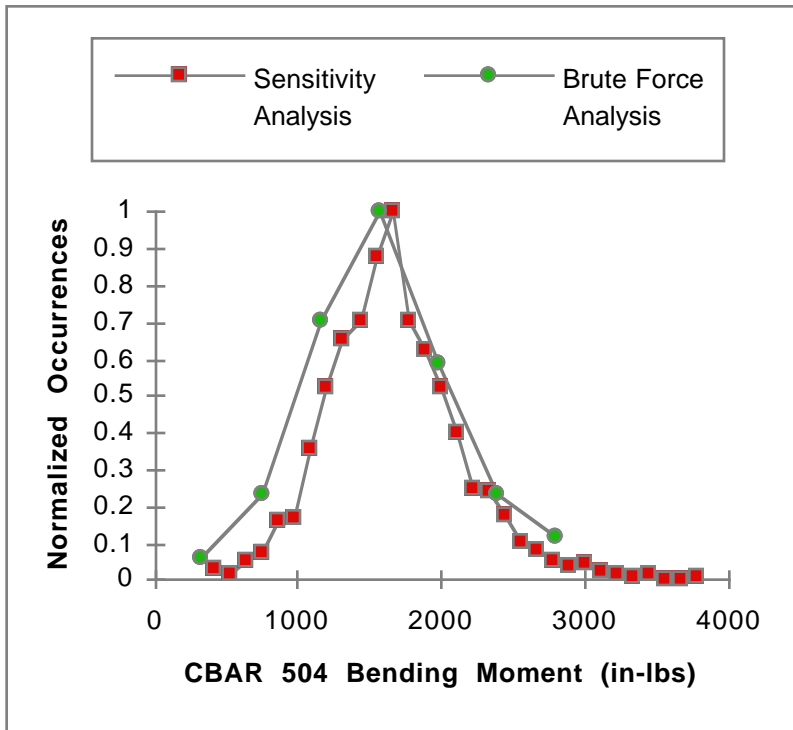


Figure 10: CBAR 504 Bending Moment Comparison Histograms from Sensitivity Analysis and Brute Force Analysis

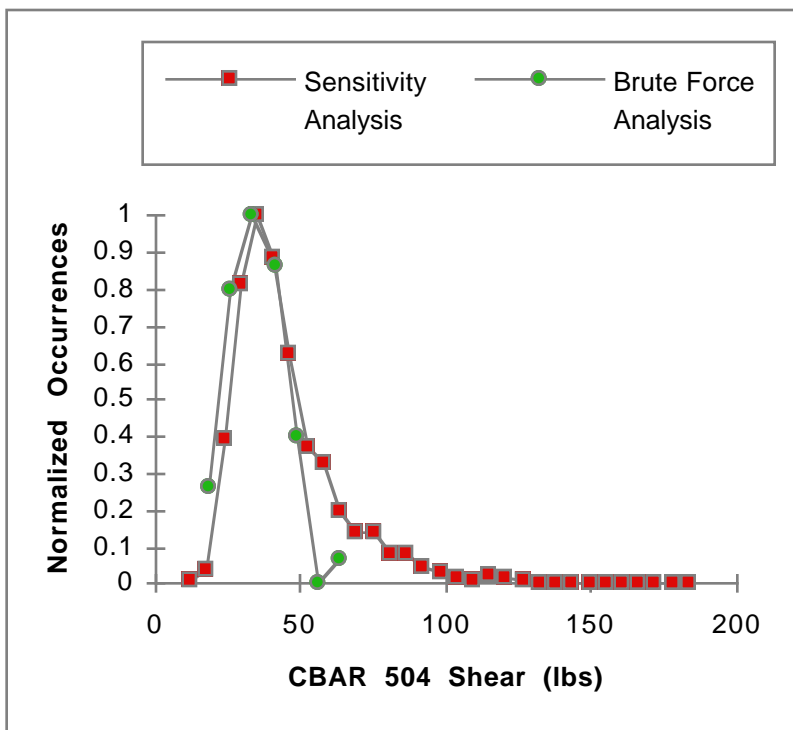


Figure 11: CBAR 504 Shear Comparison Histograms from Sensitivity Analysis and Brute Force Analysis

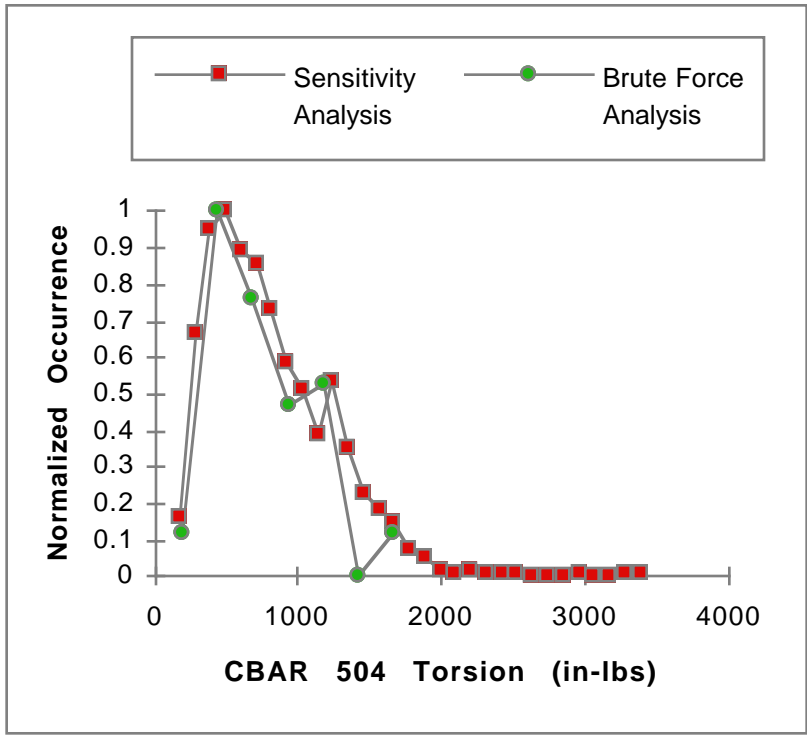


Figure 12: CBAR 504 Torsion Comparison Histograms from Sensitivity Analysis and Brute Force Analysis